

Michalis Mazonakis
Antonis Tzedakis
John Damilakis
Nicholas Gourtsoyiannis

Thyroid dose from common head and neck CT examinations in children: is there an excess risk for thyroid cancer induction?

Received: 10 May 2006
Revised: 12 July 2006
Accepted: 1 August 2006
Published online: 21 September 2006
© Springer-Verlag 2006

M. Mazonakis (✉) · A. Tzedakis
Department of Medical Physics,
Division of Radiology,
University Hospital of Iraklion,
P.O. Box 1352, 71110
Iraklion, Crete, Greece
e-mail: mazonak@med.uoc.gr
Tel.: +30-2810-392342
Fax: +30-2810-542095

J. Damilakis
Department of Medical Physics,
Faculty of Medicine,
University of Crete,
Iraklion, Crete, Greece

N. Gourtsoyiannis
Department of Radiology,
Faculty of Medicine,
University of Crete,
Iraklion, Crete, Greece

Abstract This study was conducted to estimate thyroid dose and the associated risk for thyroid cancer induction from common head and neck computed tomography (CT) examinations during childhood. The Monte Carlo N-particle transport code was employed to simulate the routine CT scanning of the brain, paranasal sinuses, inner ear and neck performed on sequential and/or spiral modes. The mean thyroid dose was calculated using mathematical phantoms representing a newborn infant and children of 1 year, 5 years, 10 years and 15 years old. To verify Monte Carlo results, dose measurements were carried out on physical anthropomorphic phantoms using thermoluminescent dosimeters (TLDs). The scattered dose to thyroid from head CT examinations varied from 0.6 mGy to 8.7 mGy depending upon the scanned

region, the pediatric patient's age and the acquisition mode used. Primary irradiation of the thyroid gland during CT of the neck resulted in an absorbed dose range of 15.2–52.0 mGy. The mean difference between Monte Carlo calculations and TLD measurements was 11.8%. Thyroid exposure to scattered radiation from head CT scanning is associated with a low but not negligible risk of cancer induction of 4–65 per million patients. Neck CT can result in an increased risk for development of thyroid malignancies up to 390 per million patients.

Keywords Computed tomography · Children · Thyroid dose · Cancer risk

Introduction

Computed tomography (CT) represents 11% of all diagnostic radiology procedures but it contributes to almost 67% of the total effective dose to the human population [1]. Pediatric CT usage has rapidly increased, and it accounts for 11% of all scans [2]. This is mainly attributed to the advent of helical CT that allows fast image acquisition and reduces dramatically the need for sedation. Head CT examinations are commonly performed in pediatric patients. Mettler et al. [2] reported that over one-third of all CT scans are in the regions of the head and neck.

Children are ten-times more sensitive to the detrimental effects of ionizing radiation than are middle-aged adults

[3]. The thyroid gland of children is an organ of very high susceptibility for radiation carcinogenesis [4]. Only a few studies have reported thyroid dose values from head and neck CT in children [5–7]. Fearon and Vunich [5] provided thyroid doses to a single patient aged 6 years, whereas Zankl et al. [6] reported dosimetric data for a neonate and a 7-year-old child. Brenner et al. [7] presented thyroid dose as a function of patient age. All the above dosimetric results were limited to the standard CT examination of the brain performed on conventional scanners.

The objectives of the current study were to estimate: (a) the thyroid dose and (b) the associated risk for thyroid cancer induction in children undergoing common head and neck examinations on multidetector CT scanners.

Materials and methods

Monte Carlo simulation

The general purpose, three-dimensional, general geometry, Monte Carlo N-particle (MCNP, version 4C2) transport code was employed to model the Siemens Somatom Sensation 16 CT scanner (Siemens, Germany). CT scans were simulated by using a linear source that rotated around the scanned region and emitted X-rays in a direction perpendicular to the source axis [8]. An incident energy spectrum of an X-ray beam at 120 kVp, suitable for the MCNP input file, was obtained from a previous study by Boone and Seibert [9]. The HVL layer of the photon beam was 7.5 mm Al at 120 kVp. Mathematical phantoms representing the body dimensions and full-scatter geometry of a newborn infant and a child of 1 year, 5 years, 10 years and 15 years old were employed (Table 1). The phantoms were generated by the commercially available BodyBuilder software (White Rock Science, N.M., USA). The generated pediatric models were based on data provided by Eckerman et al. [10].

For all mathematical phantoms, the MCNP code was used to simulate the four most common head and neck CT examinations performed in pediatric patients in our department. The scattered dose to the thyroid gland was calculated for CT scanning of the brain, paranasal sinuses and inner ear. Spiral mode is currently used for studies of the paranasal sinuses, whereas brain and inner ear scanning can be performed on both sequential and spiral acquisition modes [11]. The radiation dose received by the thyroid from the primary irradiation of the gland during spiral CT of the neck was also calculated. The scanning parameters of the CT protocols are shown in Table 2 [11]. For all CT examinations, the typical mAs values used in clinical practice at each patient age are presented in Table 3. In spiral CT, interpolation algorithms need to acquire data beyond the boundaries of the imaged volume. Therefore, additional tissue layers above and below the imaged volume are exposed by X-ray beams [8]. This extra exposure from overscanning along the phantom z-axis was taken into account for dosimetric calculations. For spiral scanning of the brain, sinuses, inner ear and neck, the

Table 1 Weight and height of the children simulated by mathematical and physical anthropomorphic phantoms

Phantom	Age (years)	Weight (kg)	Height (cm)
Mathematical	0	3.58	51.04
	1	9.71	74.57
	5	19.99	109.30
	10	33.79	139.97
	15	57.73	168.41
Physical	5	19.00	110.00
	10	32.00	140.00

z-overscanning was equal to 16 mm, 10 mm, 2 mm and 22.5 mm, respectively. The energy deposited in an anatomical area corresponding to the thyroid gland was determined using an MCNP f6 tally. The density of the thyroid corresponded to that of soft tissue and was equal to 1.04 g per cm³. For each run, 150 million histories were required to ensure a relative statistical error below 1%.

Monte Carlo simulations provided the mean thyroid dose normalized to computed tomography dose index (CTDI)_{free in air}. The normalized dose values were expressed as (mGy)_{thyroid}/(mGy)_{free in air}. To convert the normalized doses to thyroid doses in milliGrays, we used the typical mAs values shown in Table 3 and CTDI_{free in air} measurements. The CTDI_{free in air} was determined with an MDH electrometer and a 100 mm pencil ionization chamber (MDH Industries, Monrovia, Calif., USA). For beam collimations of 4×4.5 mm, 16×1.5 mm, 16×0.75 mm and 2×0.6 mm, the CTDI_{free in air} per 100 mAs was 26.06 mGy, 26.05 mGy, 29.57 mGy and 35.50 mGy, respectively.

Risk estimation for thyroid cancer induction

To estimate the risk for thyroid cancer induction in pediatric patients undergoing head and neck CT scans, we multiplied thyroid dose values in milliGrays, derived from Monte Carlo simulations, by the appropriate risk coefficient. Previous reports by the International Commission on Radiological Protection [3] and the National Council on Radiation Protection and Measurements [12] have recommended a lifetime risk for thyroid cancer induction of 0.75×10⁻² per Gy delivered by the radiosensitive gland. All risk estimations of this study express the excess of thyroid malignancies over those naturally presenting in the human population.

Thermoluminescent dosimeter measurements

Additional experiments were carried out to measure directly the thyroid dose from all head and neck CT examinations performed in sequential and/or spiral acquisition modes. Lithium fluoride thermoluminescent dosimeters (TLD-100, Harshaw, OH) 3.0×3.0×0.9 mm³ were used. Readouts were obtained on a Harshaw 3500 reader (Harshaw, Ohio, USA). The TLDs were annealed for 1 h at 400°C followed by 18 h at 80°C before the measurements were taken. For calibration, the dosimeters were exposed simultaneously to a 3 cm³ ionization chamber (Radcal Corporation, Calif., USA) in an X-ray beam resulting from 120 kVp tube voltage. The overall uncertainty of the TLD measurements was 8%.

The crystals were placed on two tissue-equivalent pediatric anthropomorphic phantoms (Atom Ltd, Norfolk, Va., USA). The weights and heights of the physical phan-

Table 2 Scanning parameters of pediatric CT protocols

Parameter	Brain, sequential	Brain, spiral	Sinuses, spiral	Inner ear, sequential	Inner ear, spiral	Neck, spiral
kV	120	120	120	120	120	120
Effective mAs	90–320	90–320	40–100	40–120	40–120	40–150
Beam collimation (mm)	4×4.5	16×1.5	16×0.75	2×0.6	2×0.6	16×1.5
Slice width (mm)	4.5	4.0	3.0	0.6	0.6	6.0
Feed/rotation (mm)	18	16.2	6.1	1.0	1.2	18.0
Rotation time (s)	0.75	0.75	0.75	0.75	0.75	0.75
Pitch	1	0.675	0.508	0.833	1	0.75

toms are shown in Table 1. The phantoms were sectional in design and manufactured with a 2.5 cm slab thickness. Each section contained a 1.5 cm×1.5 cm hole grid. The prefabricated 5 mm diameter holes allowed accommodation of the TLDs. Dose measurements were carried out on phantom section no. 8, which corresponded to the thyroid location. The TLDs were positioned in two holes located 1.5 cm on either side of the phantom midline and at a depth of 1.5–2 cm from the anterior neck surface. Two crystals were placed in each hole. The average value of the four TLD readings was taken as the thyroid dose.

Results

The scattered dose to the thyroid from CT examinations of the brain, paranasal sinuses and inner ear versus the age of the child is presented in Figs. 1, 2 and 3, respectively. Thyroid dose attributable to the primary irradiation of the gland from spiral CT of the neck is shown in Fig. 4. All the dose values obtained by Monte Carlo calculations were normalized to $CTDI_{free\ in\ air}$. As expected, a thyroid gland located inside the scanned region received a much higher dose than that associated with thyroid exposure to scattered radiation. For all CT examinations, the increase of the pediatric patient's age resulted in a reduction of the normalized thyroid dose. The scattered dose to the thyroid from CT scanning of the brain, sinuses and inner ear was strongly dependent upon the patient's age because of the age-related variations in the distance between the thyroid gland and the scanned region. The normalized thyroid dose

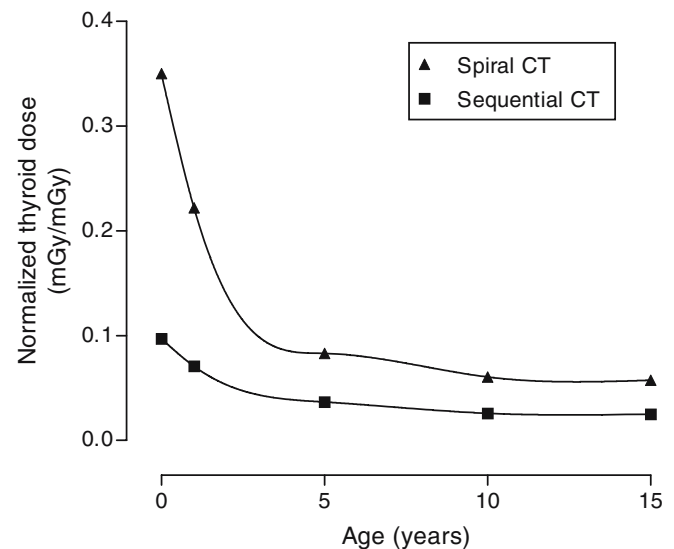
Table 3 Effective mAs values used for head and neck CT examinations in children

Effective mAs				
Age (years)	Brain, sequential/spiral	Sinuses, spiral	Inner ear, sequential/spiral	Neck, spiral
0	90	40	40	40
1	150	40	40	40
5	220	60	60	60
10	320	100	120	90
15	320	100	120	150

associated with the exposure of the gland to the primary beam during CT of the neck presented a limited variation with the age of the patient. For brain and inner ear studies, the use of sequential or spiral scanning affected the scattered dose to the thyroid gland. Based on Monte Carlo simulations, CT examination of the brain performed in spiral mode resulted in a normalized thyroid dose 2.3–3.6 times higher, depending upon the age of the child, than that obtained in sequential mode. In contrast, sequential CT of the inner ear increased the thyroid dose by a factor of up to 1.1 in comparison with the dose from spiral scanning.

For each patient age, thyroid dose values in milliGrays from all CT examinations, as derived by Monte Carlo calculations, are presented in Table 4. The mean scattered dose received by the thyroid gland varied from 0.6 mGy to 8.7 mGy, depending upon the scanned region, the acquisition mode employed and the age of the pediatric patient. Thyroid exposure to the primary beam resulted in a dose range of 15.2–52.0 mGy. The difference between the Monte Carlo calculations and TLD measurements was 6.3% to 19.8%, with a mean difference of 11.8%.

The excess lifetime risk for induction of thyroid cancer is shown in Table 5. For each CT examination, the range of

**Fig. 1** Thyroid dose normalized to $CTDI_{free\ in\ air}$ from spiral and sequential CT scanning of the brain

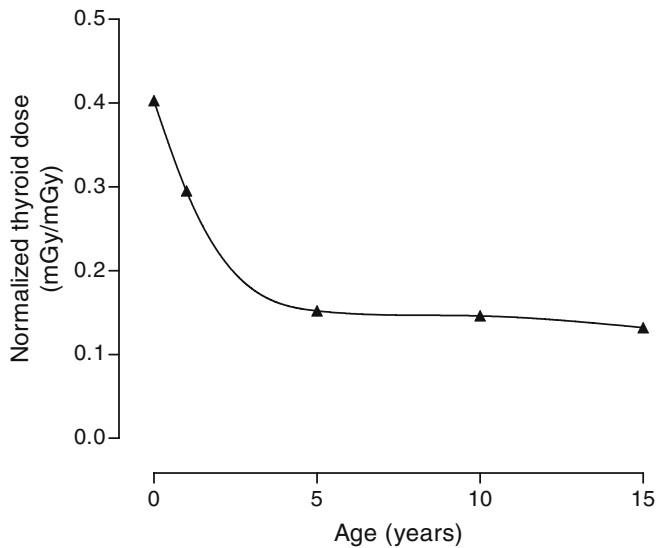


Fig. 2 Thyroid dose normalized to $CTDI_{free\ in\ air}$ from spiral CT scanning of the paranasal sinuses

risk values presented in the above table is that between the minimum and the maximum risk corresponding to the highest and lowest thyroid dose in milliGrays. For a thyroid gland located outside the imaged volume, the risk for development of thyroid malignancies from head CT scans was estimated to be $(4-65) \times 10^{-6}$. When the radiosensitive gland was included in the scanned region, the corresponding risk increased to $(114-390) \times 10^{-6}$.

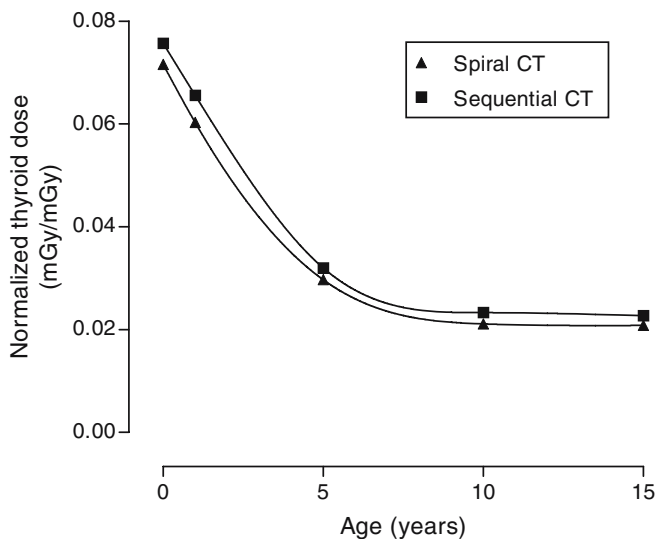


Fig. 3 Thyroid dose normalized to $CTDI_{free\ in\ air}$ from spiral and sequential CT scanning of the inner ear

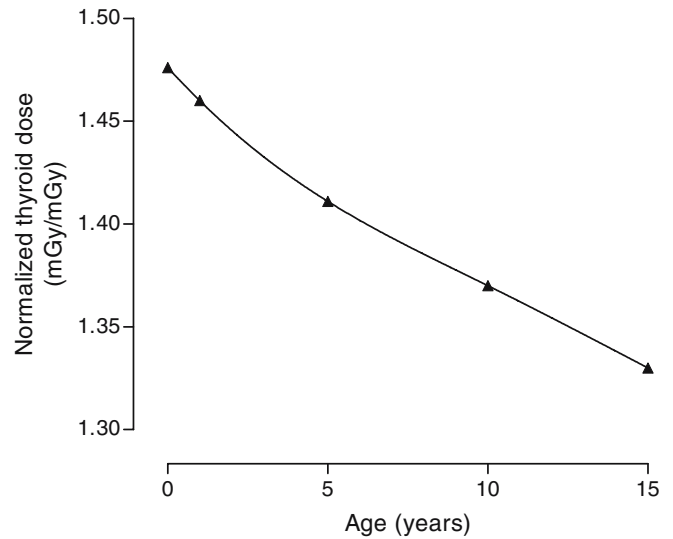


Fig. 4 Thyroid dose normalized to $CTDI_{free\ in\ air}$ from spiral CT scanning of the neck

Discussion

Monte Carlo methodology was employed to simulate four common head and neck CT examinations in children. The mean thyroid dose from CT scanning of the brain, paranasal sinuses, inner ear and neck performed in sequential and/or spiral acquisition modes was calculated. For each CT scanning, a graphical dataset showing the variation of the thyroid dose normalized to $CTDI_{free\ in\ air}$ with the age of the child is presented. These dosimetric data may be of value for thyroid dose estimation in children undergoing head and neck CT examinations on multi-detector scanners, taking into account the effects of the scanned region, the pediatric patient's age and the acquisition mode used.

Monte Carlo experiments showed that the use of a spiral CT protocol for routine studies of the brain can result in a much higher thyroid dose than that associated with sequential CT. The increase in the scattered dose could be attributed both to the z-overscanning and to the high pitch value employed during spiral CT. The z-overscanning magnitude is affected by the scanning parameters selected, including beam collimation, reconstruction slice width and pitch [8]. Further research is required to investigate whether the above parameters used during routine spiral scanning of the brain can be modified in order to restrict the z-overscanning without a significant loss of image quality.

Spiral CT examination of the inner ear reduced the thyroid dose up to 10% in comparison with the scattered dose from sequential scans. The dose reduction is mainly associated with the pitch value used. Sequential scanning of the inner ear is performed in every day clinical practice with a low pitch value compared with the pitch used for spiral studies. The z-overscanning associated with spiral CT of the inner ear is very small and equal to 2 mm. Such

Table 4 Thyroid dose in milliGrays from head and neck CT examinations in children

Thyroid dose (mGy)						
Age (years)	Brain, sequential	Brain, spiral	Sinuses, spiral	Inner ear, sequential	Inner ear, spiral	Neck, spiral
0	2.3	8.2	4.8	1.1	1.0	15.4
1	2.8	8.7	3.5	0.9	0.9	15.2
5	2.1	4.8	2.7	0.7	0.6	22.1
10	2.2	5.0	4.3	1.0	0.9	32.1
15	2.1	4.8	3.9	1.0	0.9	52.0

limited z-overscanning cannot influence significantly the dose received by the tissues excluded from the scanned region.

Recent studies have reported useful information concerning the patient dose reduction from multislice CT [13–15]. Automatic tube current modulation is a valuable tool to reduce exposure to body regions with non-circular cross-sections, where the X-ray beam attenuation varies considerably from projection to projection. Further studies are needed to investigate whether the use of mA modulation can result in a considerable thyroid dose reduction during head and neck CT scans in pediatric patients.

TLD measurements on physical humanoid phantoms were carried out to test the efficacy of Monte Carlo simulations. Dosimetric calculations presented a reasonable agreement with thyroid dose measurements, with a mean difference of 11.8%. The above discrepancy should be due to the uncertainty existing in TLD dosimetry, to the statistical errors related to Monte Carlo calculations and to the differences in size and composition between mathematical and physical phantoms. Moreover, it should be noted that Monte Carlo provided the mean scattered dose in an area corresponding to the thyroid gland, whereas TLD measurements were used to determine the scattered dose at the middle level of the radiosensitive gland.

Limited information has been reported regarding the risk for thyroid cancer induction from X-ray examinations during childhood. Most of the studies dealing with radiation risks from pediatric procedures have given an overall lifetime fatal cancer risk based on effective dose calculations rather than considering the risks for selected organs including the thyroid gland [16–18]. Brenner et al. [7] performed cancer risk assessments on an organ-by-

organ basis and summed up the organ risks. They reported that the lifetime risk for carcinogenesis from head CT in children is dominated by brain malignancies, with a contribution of approximately 10% from thyroid cancer. Their assessments of thyroid cancer induction are similar to those presented here for scanning of the brain.

Monte Carlo simulations showed that brain CT in children can result in a maximum excess incidence for thyroid cancer of 65 per million patients. The maximum risk associated with CT of the paranasal sinuses and inner ear was 36 per million patients and 8 per million patients, respectively. The above relatively low cancer risk values cannot be ignored. The CT-related risk for development of thyroid malignancies should be considered as low but not negligible whenever the radiosensitive gland is located outside the imaged volume. However, primary thyroid irradiation is associated with an increased risk for cancer induction of up to 390 per million children undergoing CT of the neck. It is well known that all diagnostic examinations requiring the use of ionizing radiation involve a risk for carcinogenesis that should be balanced against the benefit to the patient. The estimated risk values for thyroid cancer are outweighed by the potential benefits associated with head and neck CT examinations in children, whenever these radiological procedures are adequately justified. Reported experience has stated that 39% of patients who undergo head CT will have one more scan in the same region [2]. For pediatric patients needing multiple head and neck CT scans, the risk magnitude for thyroid cancer induction can be assessed using the data of this study. Risk assessment allows both the radiologists and the medical physicists to select the more dose-efficient pediatric CT protocol.

Table 5 Lifetime risk for thyroid cancer induction from head and neck CT examinations in children

CT examination	Risk ($\times 10^{-6}$)
Brain, sequential	16–21
Brain, spiral	36–65
Sinuses, spiral	20–36
Inner ear, sequential	5–8
Inner ear, spiral	4–7
Neck, spiral	114–390

Conclusion

Monte Carlo modeling can be used for calculation of sufficient thyroid dose to pediatric patients undergoing CT of the brain, paranasal sinuses, inner ear and neck with multidetector scanners. Thyroid exposure to the primary beam during CT of the neck is related to an increased risk of cancer induction. The scattered dose to the thyroid resulting from head CT scanning is not insignificant, and it can lead to a low but not negligible risk for development of

thyroid malignancies. This study presents a dataset of normalized thyroid doses that enable reasonable assessment to be made of the associated cancer risk from common pediatric CT examinations of the head and neck.

References

1. International Commission on Radiological Protection (2000) Managing patient dose in computed tomography. ICRP publication 87. Pergamon Press, Oxford
2. Mettler FA, Wiest PW, Locken JA, Kelsey CA (2000) CT scanning: patterns of use and dose. *J Radiol Prot* 20:353–359
3. International Commission on Radiological Protection (1990) Recommendations of the International Commission on Radiological Protection. ICRP publication 60. Pergamon Press, Oxford
4. Hall EJ (2000) Radiobiology for the radiologist, 5th edn. Lippincott Williams & Wilkins, Philadelphia
5. Fearon T, Vunich J (1987) Normalized pediatric organ-absorbed doses from CT examinations. *AJR Am J Roentgenol* 148:171–174
6. Zankl M, Panzer W, Petousi-Henb N, Drexler G (1995) Organ doses for children from computed tomographic examinations. *Radiat Prot Dosimetry* 57:393–396
7. Brenner DJ, Elliston CD, Hall EJ, Berdon WE (2001) Estimated risks of radiation-induced fatal cancer from pediatric CT. *AJR Am J Roentgenol* 176:289–296
8. Tzedakis A, Damilakis J, Perisinakis K, Stratakis J, Gourtsoyiannis N (2005) The effect of z overscanning on patient effective dose from multidetector helical computed tomography examinations. *Med Phys* 32:1621–1629
9. Boone JM, Seibert JA (1997) An accurate method for computer-generating tungsten anode X-ray spectra from 30 to 140 kV. *Med Phys* 24:1661–1670
10. Eckerman KF, Cristy M, Ryman JC (1996) The ORNL mathematical phantom series. Oak Ridge National Laboratory, Oak Ridge, Tenn
11. Siemens (2002) SOMATOM Sensation 16 application guide: routine protocols. Siemens, Forchheim
12. National Council on Radiation Protection and Measurements (1985) Induction of thyroid cancer by ionizing radiation. NCRP report 80. NCRP Publications: Bethesda, Maryland
13. Hohl C, Muhlenbruch G, Wildberger JE, Leidecker C, Suss C, Schmidt T, Gunther RW, Mahnken AH (2006) Estimation of radiation exposure in low-dose multislice computed tomography of the heart and comparison with a calculation program. *Eur Radiol* 16:1841–1846
14. Theocharopoulos N, Perisinakis K, Damilakis J, Karampekios S, Gourtsoyiannis N (2006) Dosimetric characteristics of a 16-slice computed tomography scanner. *Eur Radiol Apr* 22; [Epub ahead of print] DOI <http://dx.doi.org/10.1007/s00330-006-0251-0>
15. Vock P (2005) CT dose reduction in children. *Eur Radiol* 15:2333–2340
16. Bacher K, Bogaert E, Lapere R, De Wolf D, Thierens H (2005) Patient-specific dose and radiation risk estimation in pediatric cardiac catheterization. *Circulation* 111:83–89
17. Mazonakis M, Damilakis J, Raissaki M, Gourtsoyiannis N (2004) Radiation dose and cancer risk to children undergoing skull radiography. *Pediatr Radiol* 34:624–629
18. Perisinakis K, Raissaki M, Damilakis J, Stratakis J, Neratzoulakis J, Gourtsoyiannis N (2006) Fluoroscopy-controlled voiding cystourethrography in infants and children: are the radiation risks trivial? *Eur Radiol* 16:846–851